Dimerization and fusion of C_{60} molecules caused by molecular collision

Yueyuan Xia, Yuelin Xing, Chunyu Tan, and Liangmo Mei
Department of Physics, Shandong University, Jinan, Shandong 250100, China
(Received 14 August 1995; revised manuscript received 13 December 1995)

Collisions between two C_{60} molecules are studied using molecular dynamics simulations. The results show that dumbbell-shaped $(C_{60})_2$ dimers with almost intact cages can be formed at low collision energies, and when the collision energy is high enough to overcome the fusion barrier, the two colliding C_{60} molecules fuse to form one large C_{120} cluster. These coalescence reactions are found to have very clear threshold behavior. The threshold energy of dimerization is dependent on the classical impact parameter between the mass centers of the colliding partners, and on the collisional orientation. The coalescence reactions are shown to be deep inelastic. The total cross section for the coalescence reaction is estimated to be on the order of the area of a circle, that has a radius equal to the diameter of a C_{60} molecule. [S0163-1829(96)04820-5]

I. INTRODUCTION

Molecular fusion of C_{60} molecules caused by C_{60}^+ ion and C_{60} molecule collision has been studied experimentally and theoretically.[1,2] Coalescence reactions of C_{60} molecules resulting from molecular collisions in the vapors generated by laser desorption of fullerene films and from impact of C_{60}^+ ions on crystalline fullerite targets have also been reported.[3,4] These studies can provide important information on the growth mechanism of larger fullerenes and basic understanding of the field of fullerene chemistry. Although the experimental evidence for molecular coalescence of C_{60} molecules is clearly manifested by measurements of the mass spectra, the shapes of the products from the coalescence reactions are not clearly known. For example, it is not clear whether the coalescence product is formed as one large cluster or is a dumbbell-shaped $(C_{60})_2$ dimer. Also, it is not known how the coalescence reaction depends on the collision energy and on the classical impact parameter between the colliding partners, and what is the threshold energy for the reaction. Molecular dynamics simulations are particularly suitable to give answers to these questions. Therefore, they have often been used to simulate cluster-cluster collisions.[2,5] In the present work, we use a molecular dynamics simulation method to study the detailed processes of dimerization and fusion reactions induced by two-C_{60} collisions.

In order to obtain detailed information, we need a very time-efficient simulation method. An empirical potential, developed by Brenner[6] according to the Abell-Tersoff bonding formalism,[7–10] is used in the simulations, rather than using an *ab initio* potential, to avoid too intensive simulation calculations. The transferability of this potential has been tested and proved to be good in modeling the process of C_{60} collision with a hydrogen-terminated diamond surface,[11] the formation of endohedral complexes of fullerenes,[12] and the formation, via the curling and closure of graphite ribbons, of hollow structures representing fullerene precursors.[13] The interatomic potential and the simulation results will be given in the following sections.

II. INTERATOMIC POTENTIAL AND SIMULATION METHOD

An empirical combination potential is chosen to describe the interatomic interactions for two colliding C_{60} molecules. The potential is given by

$$V(r_{ij}) = f_c(r_{ij}) V_{\mathrm{BZ}}(r_{ij}) + [1 - f_c(r_{ij})] V_{\mathrm{TB}}, \tag{1}$$

where r_{ij} is the distance between atom i and atom j, $V_{\mathrm{BZ}}(r_{ij})$ is the universal potential given by Biersack and Ziegler,[14,15] which is used to model hard-core behavior for close-distance collisions, V_{TB} is the Brenner potential[6] used here to describe the many-body potential among C atoms, and $f_c(r_{ij})$ is a combination coefficient used to spline the hard-core potential $V_{\mathrm{BZ}}(r_{ij})$ and the Brenner potential V_{TB}. The combination coefficient $f_c(r)$ is given by

$$f_c(r) = \begin{cases} 1 & \text{for} \quad r \leq R_r \\ \cos^2\left[\dfrac{\pi(r - R_r)}{2(R_a - R_b)}\right] & \text{for} \quad R_r < r \leq R_a, \\ 0 & \text{for} \quad r > R_a, \end{cases} \tag{2}$$

where R_a is determined by the condition $V_{\mathrm{TB}}(R_a) = 0$, and R_r is taken as $R_r = 0.1 R_a$.

The universal potential is given by

$$V_{\mathrm{BZ}}(r) = V(r)[A_1 \exp(-B_1 x) + A_2 \exp(-B_2 x) + A_3 \exp(-B_3 x) + A_4 \exp(-B_4 x)], \tag{3}$$

where $x = r/a$, a is the screening radius, and $V(r)$ is the Coulomb potential. The coefficients in the screening function, A_1, A_2, A_3, A_4, B_1, B_2, B_3, and B_4, and the screening radius a are given in Ref. 15. The Brenner potential $V_{\mathrm{TB}}(r)$ is actually a highly parametrized version of Tersoff's empirical-bond-order formalism, but it includes terms that correct for an inherent overbinding of radicals and incorporates nonlocal effects, and therefore is an improved Tersoff-type potential. It is given by

$$V_{\mathrm{TB}}=\sum_i \sum_{j(>i)} [V_R(r_{ij})-\overline{B_{ij}}V_A(r_{ij})], \tag{4}$$

where the repulsive pair potentials are given by

$$V_R(r_{ij})=f_{ij}(r_{ij})\frac{D_{ij}}{(S_{ij}-1)}\exp[-\sqrt{2S_{ij}}\beta_{ij}(r_{ij}-R_{\mathrm{CC}})], \tag{5}$$

where D_{ij} is the well-depth parameter, R_{CC} is an equilibrium distance, S_{ij} is a parameter used to make the potential Morse-type pairlike (if $S_{ij}=2$, then the pair terms reduce to the usual Morse potential), and the parameter β_{ij} is equal to the usual Morse parameter independent of the value of S_{ij}. The attractive pair terms are given by

$$V_A(r_{ij})=f_{ij}(r_{ij})\frac{D_{ij}S_{ij}}{(S_{ij}-1)}\exp\left[-\left(\frac{2}{S_{ij}}\right)^{1/2}\beta_{ij}(r_{ij}-R_{\mathrm{CC}})\right]. \tag{6}$$

The cutoff function $f_{ij}(r_{ij})$ is given by

$$f_{ij}(r)=\begin{cases}1 & \text{for} \quad r\leqslant R^{(1)},\\ 0.5+0.5\cos\left[\dfrac{\pi(r-R^{(1)})}{(R^{(2)}-R^{(1)})}\right] & \text{for} \quad R^{(1)}<r\leqslant R^{(2)},\\ 0 & \text{for} \quad r>R^{(2)},\end{cases} \tag{7}$$

where $R^{(1)}$ and $R^{(2)}$ are distances chosen to restrict the distance of the interaction. An unusual feature of the potential is that it has a bond-order function $\overline{B_{ij}}$ which represents a many-body coupling between the bond from atom i to atom j and the local environment of atom i.[6,8–10] The bond-order function appearing in Eq. (4) is given by

$$\overline{B_{ij}}=(B_{ij}+B_{ji})/2+F_{ij}(N_i^{(t)},N_j^{(t)},N_{ij}^{\mathrm{conj}}), \tag{8}$$

$$B_{ij}=\left[1+\sum_{k\neq(i,j)} G_i(\theta_{ijk})f_{ik}(r_{ik})\right]^{-p_i}, \tag{9}$$

where $N_i^{(t)}$ and $N_j^{(t)}$ are the total number of neighbors of atom i and atom j, respectively, N_{ij}^{conj} is used to determine whether a C-C bond is part of a conjugated system and is defined by Eqs. (15)–(17) of Ref. 6, θ_{ijk} is the bond angle between bond r_{ij} and r_{ik}, $F_{ij}(N_i^{(t)},N_j^{(t)},N_{ij}^{\mathrm{conj}})$ is used as a correction function, and p_i is a parameter. $G_i(\theta_{ijk})$ is given by

$$G_i(\theta_{ijk})=a_0\left\{1+\frac{c_0^2}{d_0^2}-\frac{c_0^2}{[d_0^2+(1+\cos\theta_{ijk})^2]}\right\}, \tag{10}$$

where a_0, c_0, and d_0 are parameters. Some values of $F_{ij}(N_i^{(t)},N_j^{(t)},N_{ij}^{\mathrm{conj}})$ and the partial derivatives used to interpolate F_{ij} values, and all the parameters in Eqs. (4)–(10), can be found from Tables I and III of Ref. 6. Parameters for potential I of Ref. 6 are used in the present work. As mentioned above, the transferability of this potential has been extensively tested. Furthermore, we have used this potential to simulate the structural and energetic behavior of the C_{60} molecule. The average diameter of the C_{60} cage obtained by the potential is 7.13 Å, which agrees very well with the result of 7.1 Å obtained from an *ab initio* molecular dynamics simulation.[16] The average lengths of single bond and double bond are 1.449 and 1.419 Å, respectively. The values are in good agreement with the experimental data,[17,18] *ab initio* calculation results,[16,19] and the result from a tight-binding molecular dynamics simulation.[20] The cohesive energy per atom in the C_{60} cage predicted by the potential is -7.04 eV, which should be about 0.4 eV below (less stable than) the cohesive energy per atom in graphite.[3] The experimental value of the cohesive energy per atom in graphite is found to be -7.427 eV. The successful description of the structural and energetic properties of the C_{60} molecule using this potential further proves that the potential has very good transferability since all the parameters of the potential are determined[6] without consideration of the properties of C_{60} at all.

Using the potential described above, we have simulated the collision process of two C_{60} molecules. The two C_{60} molecules are initially set to have the same orientation. Their threefold axis is set along the z axis, and their twofold axes are set along the x axis and y axis, respectively. One of them (the target) is set to be at rest, and the other one (the projectile) to have an incident velocity. The energy of the projectile and the impact parameter between the mass centers of the C_{60} molecules are changed to study the energy and impact-parameter dependence of the collision reactions. In order to study the orientational dependence of the collisional reaction channels, we have also changed the collisional direction by rotating (i.e., changing the polar angle θ and the azimuthal angle φ) the projectile randomly before the collision. The classical equations of motion for all atoms involved are integrated using a predictor-corrector method. A step size of 10^{-16} s is proved to be satisfactory to maintain conservation of energy during the whole simulation process.

III. SIMULATION RESULTS

A. Threshold energy of coalescence for two colliding C_{60} molecules

Figure 1 shows a scattering process of two C_{60} molecules. Initially, the C_{60} on the right side (the target) is at rest while the C_{60} on the left (the projectile) is set to have a laboratory incident energy $E_0=21$ eV. The two C_{60} cages have the same orientation ($\theta=0$, $\varphi=0$) and the impact parameter between the mass centers of the C_{60} molecules is $b=0$, i.e., the two C_{60} molecules have a head-on collision. At simulation time $t=70.3$ fs, the C_{60} cages encounter each other and are deformed, and some bonds connecting the projectile and the

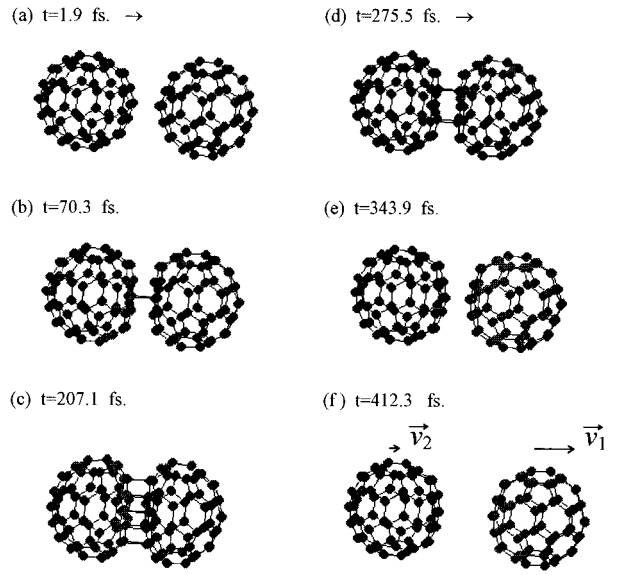

FIG. 1. Quasielastic scattering of two C_{60} molecules at incident energy $E_0=21$ eV and at impact parameter $b=0$.

target are formed. In the time interval from $t=70.3$ to 207.1 fs, the colliding partners experience a compression process with more and more connecting bonds formed. Afterwards, the deformed projectile and target rebound from each other, and at $t=343.9$ fs the two C_{60} molecules are totally separated. About 93% of the incident energy of the projectile is transferred to the target. Both the projectile C_{60} and the target C_{60} are in very low excited states, which have an average total deformation energy $E_d\sim0.756$ eV and an average total vibration internal energy $E_t\sim0.767$ eV. From this result it is obvious that the collision is nearly elastic (quasielastic) although inelastic effects also exist. However, if the incident energy is increased to $E_0=21.5$ eV, while keeping other collision conditions unchanged, we see a substantially different collision process, as shown in Fig. 2. In this case, although the two colliding partners also experience a compression and rebound process, they cannot be separated. They form a very

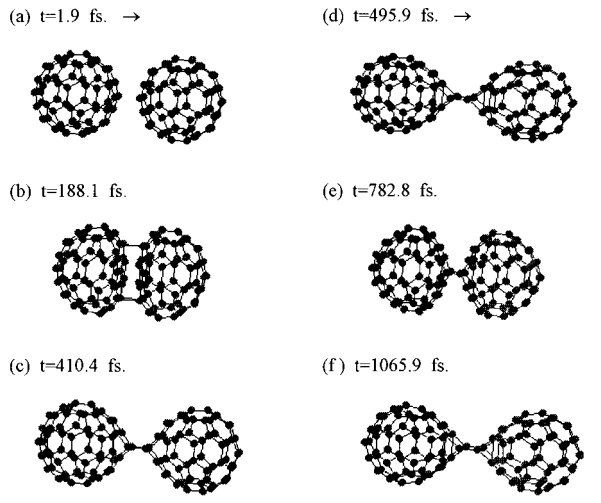

FIG. 2. Dimerization reaction induced by collision of two C_{60} molecules at incident energy $E_0=21.5$ eV and at impact parameter $b=0$.

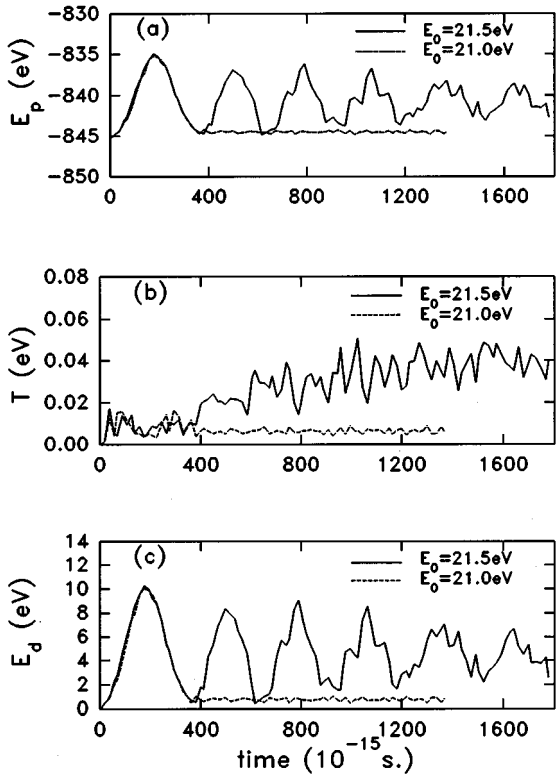

FIG. 3. The temporal evolution of the potential energy, the temperature, and the deformation energy for two C_{60} molecules colliding at energy $E_0=21.5$ eV (the solid lines) and at $E_0=21.0$ eV (the dashed lines).

stable dumbbell-shaped $(C_{60})_2$ dimer, which vibrates by compressing and expanding alternately. It is evident that the $(C_{60})_2$ dimer formed is similar to the most stable 1,2-$(C_{60})_2$ dimer structure with a D_{2h} symmetry predicted by a modified neglect of differential overlap (MNDO) and *ab initio* density functional calculation.[21] As long as the incident energy E_0 is lower than 21 eV, we always observe a quasielastic scattering of the colliding C_{60} molecules, similar to the case shown in Fig. 1. However, if the incident energy E_0 is higher than 21.5 eV, coalescence reactions of the C_{60} molecules are always observed, provided the colliding partners keep in the orientation $\theta=0$ and $\varphi=0$ before the collision takes place. Therefore we obtain the threshold energy of dimerization for two C_{60} molecules colliding at impact parameter $b=0$, which is 21.5 eV. We find that this is the lowest threshold energy for dimerization. In order to demonstrate the sudden change around the reaction threshold, in Fig. 3 we show the potential energies, the internal energies (the ''temperatures''), and the deformation energies varying with time for the collision systems given in Figs. 1 and 2, respectively. The solid lines are for the case of incident energy $E_0=21.5$ eV, and the dashed lines give the corresponding result for the case of $E_0=21.0$ eV. The top panel in the figure gives the potential energies of the two collision systems changing with time, the middle panel gives the temperatures of the systems versus time, and the bottom panel gives the time evolution of the deformation energies of the systems. It is clear that during the first stage of the collision, which takes place in a time interval of less than 400 fs, these systems have very similar collision behavior. During this pe-

riod the colliding partners are both nearly adiabatically deformed, and the ''temperature'' in this period does not have the usual meaning. It only represents the energy of motion of the C atoms relative to the mass centers of the C_{60} molecules, caused by the collision itself. The first peaks appearing around $t=180$ fs in the potential-energy curve and the deformation-energy curve give the time at which the two C_{60} molecules have the maximum compression deformation induced by the collision. Afterwards, the two C_{60} molecules rebound and the two systems have totally different behavior. In the case of $E_0=21$ eV, which is lower than the threshold energy for dimerization, the potential energy of the two quasielastically scattered C_{60} molecules almost recovers to its initial level. As a result, the two C_{60} molecules have very low internal energy (temperature) and very low deformation energy, as shown by the dashed lines in this figure. This shows the remarkable resilience of the structure of the C_{60} molecule, and indicates that the scattered C_{60} molecules are in very low excited states. The resilient behavior of C_{60} was also observed in the collision of C_{60} with the diamond surface.[11] However, in the case of $E_0=21.5$ eV, which equals the threshold energy for dimerization, the $(C_{60})_2$ dimer has much higher temperature and much higher deformation energy, which changes synchronistically with the potential energy. The oscillations of the potential energy and the deformation energy shown in this figure demonstrate the regular vibration of the $(C_{60})_2$ dimer produced, compressing and expanding alternately, as shown in Fig. 2. The temperature fluctuation around an average value of ~ 0.037 eV indicates that the $(C_{60})_2$ dimer, produced by a collision in the low-energy region, is in a low thermal excitated state and is very stable. This deep inelastic behavior manifested in the present work has also been found in experiments on coalescence reactions of C_{60} molecules,[1,4] as well as in molecular dynamics simulations for cluster collisions,[2,5] C_{60} collision with the diamond surface,[11] and C_{60} collision with He.[12]

B. Impact-parameter-dependent threshold energy for coalescence

If one changes the impact parameter of the two colliding C_{60} molecules, it is found that the threshold energy for coalescence changes with impact parameter. For example, we simulated two C_{60} molecules colliding at impact parameter $b=2.1$ Å. It is found that the coalescence reaction cannot take place as long as the laboratory incident energy is less than 52.0 eV. Figure 4 shows a collision process at incident energy $E_0=51$ eV and at impact parameter $b=2.1$ Å, while keeping $\theta=0$ and $\varphi=0$. It is evident that at first the C_{60} molecules coalesce to form a dumbbell-shaped dimer, joined together by many bonds. Then they rebound from each other, and at time $t=399$ fs, the bonds joining them are all ruptured, eventually yielding two scattered C_{60} molecules moving apart from each other. The scattered C_{60} molecules keep about 80% of the initial incident energy, and the rest of the energy becomes the deformation energy and the thermal energy within the C_{60} molecules. Therefore the inelastic component of the collision is increased in comparison with the case shown in Fig. 1. When we increase the incident energy to $E_0=52.0$ eV, while keeping the other collision conditions exactly the same as in Fig. 4, the coalescence reaction is observed, as shown in Fig. 5. From this figure, it is obvious

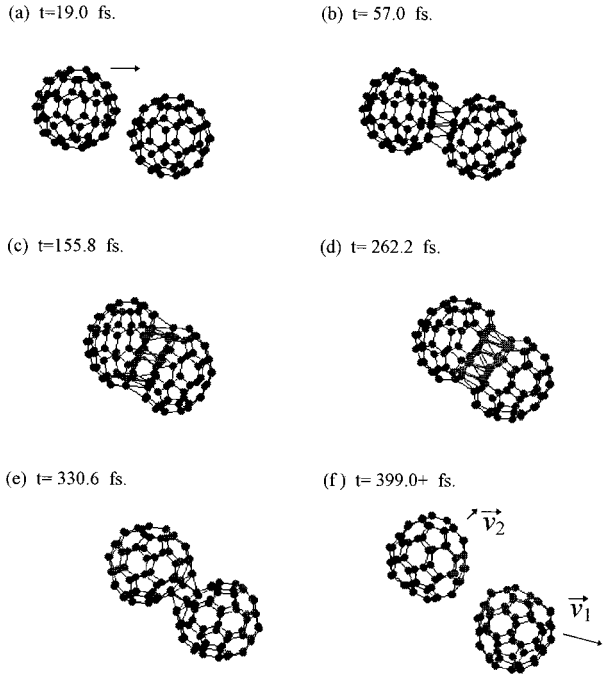

FIG. 4. Scattering process of two C_{60} molecules caused by a collision at energy $E_0=51.0$ eV and at impact parameter $b=2.1$ Å.

that a stable dumbbell-shaped $(C_{60})_2$ dimer is formed. In comparison with the dimer shown in Fig. 2, the dimer shown in Fig. 5 has more bonds joining the two C_{60} cages together. We also analyzed the potential energy, the internal heat energy, and the deformation energy for the collisions of Figs. 4 and 5. Very similar to the case shown in Fig. 3, the coalescence reaction demonstrates deep inelastic behavior. From the cases shown in Figs. 4 and 5 the threshold energy for the

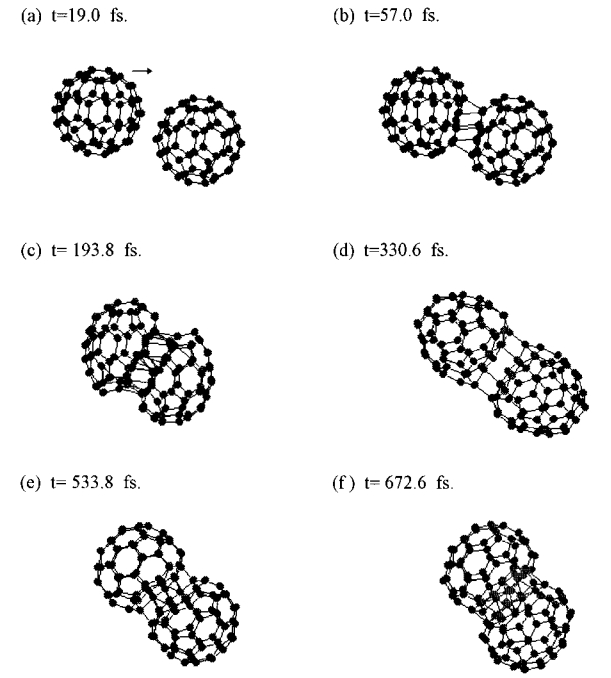

FIG. 5. Coalescence reaction induced by a collision of two C_{60} molecules at energy $E_0=52.0$ eV and at impact parameter $b=2.1$ Å.

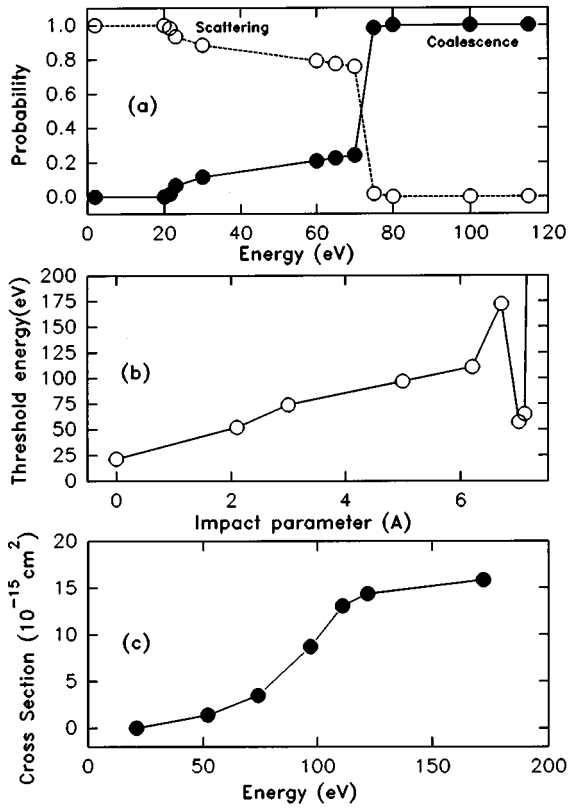

FIG. 6. (a) Probability of coalescence reaction and probability of scattering as functions of incident energy for C_{60} molecular collision at zero impact parameter; (b) threshold energy of coalescence reaction as a function of impact parameter for two C_{60} molecules colliding at $\theta=0$ and $\varphi=0$; (c) cross section of coalescence reaction as a function of collision energy for two C_{60} molecules colliding at $\theta=0$ and $\varphi=0$.

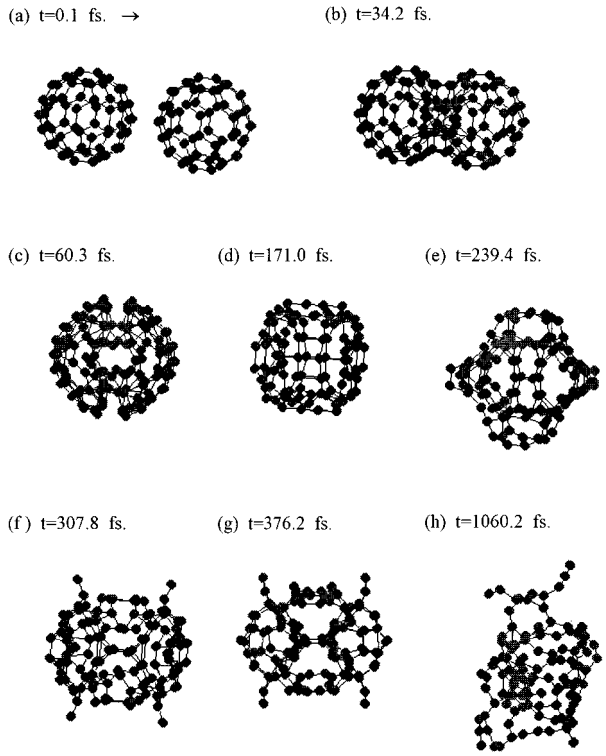

FIG. 7. Fusion reaction induced by a head-on collision of two C_{60} molecules at energy $E_0=400$ eV.

coalescence reaction is determined to be 52.0 eV for two C_{60} molecules colliding at impact parameter $b=2.1$ Å and at $\theta=0$, $\varphi=0$. In the same way, we found that the threshold energy of the coalescence reaction of two C_{60} molecules at impact parameter $b=3.0$ Å ($\theta=0$, $\varphi=0$) is increased to 74.0 eV. At larger impact parameters a remarkable rotation of the coalescence products is observed in the simulations (not shown here). By increasing the impact parameter and the incident energy continuously, we estimated the total cross section for the coalescence reaction of two colliding C_{60} molecules, and found it is about 1.58×10^{-14} cm^2. It is just about the geometrical area of a circle with a radius of 7.1 Å, the geometrical diameter of a C_{60} molecule. Changing the relative orientation of the colliding partners by rotating the projectile randomly just before the collision, we found that the threshold energy for the coalescence reaction changes remarkably. The probability for the different reaction channels can be obtained by simulations under different collisional orientations. In the top panel of Fig. 6 we show the probability of the coalescence reaction and that of scattering as functions of the collisional energy for collisions at zero impact parameter. The solid and the hollow dots shown in the figure are the results obtained by the simulations, while the curves are drawn to guide the eye. It is obvious that although the lowest threshold energy for the coalescence reaction is 21.5 eV, only when the incident energy increases to 80 eV, can the coalescence reaction take place with a probability of unity. The threshold energy as a function of impact parameter obtained by the simulations for the case of the colliding partners having the same orientation (i.e., $\theta=0$, $\varphi=0$) is shown in the middle panel of Fig. 6. It is clear that the threshold energy changes with the impact parameter b. In the bottom panel of this figure we give the cross section of the coalescence reaction, which relates to the reaction probability, as a function of collision energy for the case of $\theta=0$ and $\varphi=0$. It shows that the cross section increases with the incident energy until the maximum value of the cross section is reached.

C. Real fusion reactions

If the collision energy is high enough to overcome the fusion barrier, one cluster is really obtained. Figure 7 shows the process of two C_{60} molecules colliding at laboratory energy $E_0=400$ eV, at impact parameter $b=0$ and at a collisional orientation of $\theta=0$ and $\varphi=0$. It is obvious that these two C_{60} molecules are completely compressed together to form one cluster, completely losing the geometry of the original C_{60} cages. The fusion product, a C_{120} cluster, is highly excited. The deformation energy stored in C_{120} can go as high as 120 eV above the level of two separate C_{60} molecules. The fusion products, at first, experience a structure relaxation process, during which the shape of the C_{120} cluster stays symmetric. Afterwards, its ''temperature'' is gradually increased, and then at simulation time $t=1060.2$ fs it becomes an unsymmetric cluster, as shown in Fig. 7(h). Following a 2×10^5 time-step simulation, a C_2 dimer loss, via evaporation, to form a C_{118} cluster is observed. Then a se-

quential loss of C_2 dimers, C_3 trimers, and individual C atoms is observed. The detailed fragmentation pattern following the fusion reaction will be given elsewhere.

IV. DISCUSSION AND CONCLUSION

We have studied in detail the coalescence reactions caused by molecular collision between two C_{60} molecules using an empirical potential. The central problem of using a parametrized potential is the transferability of the potential. As mentioned in Sec. II, the transferability of the potential has been tested and proved to be very good. In summary, we have found that the coalescence reaction caused by collisions between two C_{60} molecules has very clear threshold behavior, which is dependent on the classical impact parameter and the collisional orientation. A pure dimerization reaction at low energy and at $b=0$ is observed, and the dumbbell-shaped $(C_{60})_2$ dimer produced has a structure similar to the most stable 1,2-$(C_{60})_2$ dimer predicted theoretically.[21] A pure fusion reaction is observed for a head-on collision between two C_{60} molecules at laboratory incident energy $E_0=400$ eV. Following the fusion reaction, the increasing heat energy of the fusion product leads to sequential evaporation of C_2 dimers, C_3 trimers, and individual C atoms from the cluster. The threshold energy of the coalescence reaction between two C_{60} molecules varies with the impact parameter and with the collisional orientation. If the incident energy is lower than the threshold energy the two C_{60} molecules are scattered. The inelastic component of this scattering process increases with the incident energy. All types of coalescence reactions are shown to have deep inelastic behavior. These results are consistent with the experimental results obtained by mass spectrometry experiments.[1,31]

ACKNOWLEDGMENTS

This work was supported by the National Natural Science Foundation of China.

[1] E. E. B. Campbell, V. Schyja, R. Ehlich, and I. V. Hertel, Phys. Rev. Lett. **70**, 263 (1993).
[2] G. Seifert and R. Schmidt, in *Clusters and Fullerenes*, edited by V. Kumar, T. P. Martin, and E. Tosatti (World Scientific, Singapore, 1992).
[3] C. Yeretzian, K. Hansen, F. Diederich, and R. L. Whetten, Nature **359**, 44 (1992).
[4] T. Lill, F. Lacher, Hans-Gerd Busmann, and I. V. Hertel, Phys. Rev. Lett. **71**, 3383 (1993).
[5] R. Schmidt, G. Seifert, and H. O. Lutz, Phys. Lett. A **158**, 231 (1991).
[6] D. W. Brenner, Phys. Rev. B **42**, 9458 (1990).
[7] G. C. Abell, Phys. Rev. B **31**, 6184 (1985).
[8] J. Tersoff, Phys. Rev. Lett. **56**, 632 (1986).
[9] J. Tersoff, Phys. Rev. B **37**, 6991 (1988).
[10] J. Tersoff, Phys. Rev. Lett. **61**, 2879 (1988).
[11] R. C. Mowrey, D. W. Brenner, B. I. Dunlap, J. W. Mintmire, and C. T. White, J. Phys. Chem. **95**, 7138 (1991).
[12] R. C. Mowrey, M. M. Ross, and J. H. Callahan, J. Phys. Chem. **96**, 4755 (1992).
[13] D. H. Robertson, D. W. Brenner, and C. T. White, J. Phys. Chem. **96**, 6133 (1992).
[14] J. P. Biersack and J. F. Ziegler, Nucl. Instrum. Methods **194**, 93 (1982).
[15] J. F. Ziegler, J. P. Biersack, and U. Littmark, in *The Stopping and Range of Ions In Solids*, edited by J. F. Ziegler (Pergamon, New York, 1985).
[16] Q.-M. Zhang, J.-Y. Yi, and J. Bernholc, Phys. Rev. Lett. **66**, 2633 (1991).
[17] C. S. Yannoni, P. P. Bernier, D. S. Bethune, G. Meijer, and J. R. Salem, J. Am. Chem. Soc. **113**, 3190 (1991).
[18] F. Li and J. S. Lannin, in *Proceedings of the International Symposium on the Physics and Chemistry of Finite Systems: From Cluster to Crystals*, edited by P. Jena, S. N. Khanna, and B. K. Rao (Kluwer, Boston, 1992).
[19] K. Baghavachari and C. M. Rohlfing, J. Chem. Phys. **95**, 5769 (1991).
[20] C. Z. Wang, C. T. Chan, and K. M. Ho, Phys. Rev. B **46**, 9761 (1992).
[21] N. Matzuzawa, M. Ata, D. A. Dixon, and G. Fitzgerald, J. Phys. Chem. **98**, 2555 (1994).